Compound-specific carbon isotopes from Earth's largest flood basalt eruptions directly linked to the end-Triassic mass extinction

Jessica H. Whiteside[a,1], Paul E. Olsen[b,1], Timothy Eglinton[c], Michael E. Brookfield[d], and Raymond N. Sambrotto[e]

[a]Department of Geological Sciences, Brown University, Box 1846, Providence, RI 02912; [b]Department of Earth and Environmental Sciences, Lamont-Doherty Earth Observatory of Columbia University, Palisades, NY 10964; [c]Department of Marine Geology and Geophysics, Woods Hole Oceanographic Institution, Woods Hole, MA 02543; [d]Institute of Earth Sciences Academia Sinica, Nankang, Taipei 11529, Taiwan; and [e]Lamont-Doherty Earth Observatory of Columbia University, Palisades, NY 10964

Contributed by Paul E. Olsen, February 12, 2010 (sent for review January 12, 2010)

A leading hypothesis explaining Phanerozoic mass extinctions and associated carbon isotopic anomalies is the emission of greenhouse, other gases, and aerosols caused by eruptions of continental flood basalt provinces. However, the necessary serial relationship between these eruptions, isotopic excursions, and extinctions has never been tested in geological sections preserving all three records. The end-Triassic extinction (ETE) at 201.4 Ma is among the largest of these extinctions and is tied to a large negative carbon isotope excursion, reflecting perturbations of the carbon cycle including a transient increase in CO_2. The cause of the ETE has been inferred to be the eruption of the giant Central Atlantic magmatic province (CAMP). Here, we show that carbon isotopes of leaf wax derived lipids (*n*-alkanes), wood, and total organic carbon from two orbitally paced lacustrine sections interbedded with the CAMP in eastern North America show similar excursions to those seen in the mostly marine St. Audrie's Bay section in England. Based on these results, the ETE began synchronously in marine and terrestrial environments slightly before the oldest basalts in eastern North America but simultaneous with the eruption of the oldest flows in Morocco, a CO_2 super greenhouse, and marine biocalcification crisis. Because the temporal relationship between CAMP eruptions, mass extinction, and the carbon isotopic excursions are shown in the same place, this is the strongest case for a volcanic cause of a mass extinction to date.

astrochronology | CO_2 | Jurassic | large igneous provinces | *n*-alkane

Plants record through photosynthetic pathways the atmospheric values of $\delta^{13}C$ that in turn reflect the exchangeable surface oceanic carbon reservoir (1). One of the most direct known plant proxies is the $\delta^{13}C_{alk}$ measurements of n-C_{25}–n-C_{31} *n*-alkanes derived from leaf wax lipids of plant cuticles (2). We analyzed $\delta^{13}C_{alk}$, the carbon isotopic composition of wood ($\delta^{13}C_{wood}$), and total organic carbon ($\delta^{13}C_{toc}$) from sediments from two overlapping lacustrine sections interbedded with the lavas of the Central Atlantic magmatic province (CAMP) (3) in eastern North America to obtain a carbon isotope record unambiguously tied to the eruptions and climate proxies to compare with and calibrate organic carbon and carbonate $\delta^{13}C$ records from elsewhere (3–7). This allows direct determination of the relationship between one of the largest Phanerozoic mass extinctions, the end-Triassic extinction (ETE) (8), carbon isotopic and CO_2 (9) excursions, the biocalcification crisis (10), and their proposed cause, the CAMP (3, 11–13). Core and outcrop samples were obtained from the Newark (New York, New Jersey, and Pennsylvania) and Hartford (Connecticut and Massachusetts) rift basins at 19–20° N paleolatitude (14) in the tropical humid to arid transition of central Pangea (Fig. 1). A hierarchy of Milankovitch-forced lake level cycles permeate the sampled strata in these basins, and in conjunction with a high sediment accumulation rate and magnetostratigraphic and radioisotopic calibration (*SI Text* and Datasets S1–S3), a 2.4 m.y. unbroken record of events

Fig. 1. Map of Pangea at 201 Ma showing the distribution of the CAMP and the localities discussed in the text: 1, St. Audrie's Bay; 2, Newark basin; 3, Hartford basin; 4, Kennecott Point; 5, Val Adrara; 6, Moroccan CAMP sections. Base map (orthographic projection) courtesy of C. Scotese based on the latitudinal positions of ref. 14.

surrounding the ETE can be placed into the high-precision (<20 ky) Newark/Hartford basin astronomically calibrated geomagnetic polarity time scale (NBAGPTS) (15–17) (Fig. 2). The combined section is registered to the marine record by high-resolution magnetostratigraphy (17, 18), high-precision U-Pb ages, and cyclostratigraphy (7, 19), and spans the late Rhaetian of the Late Triassic to the early Sinemurian of the Early Jurassic (Fig. 2). Our data indicate the *n*-alkanes from these strata preserve an original leaf wax signal (*SI Text*).

Carbon Isotope Results

All three sets of carbon isotopic data from the Newark and Hartford basin sections show considerable variability seemingly tied in part to the lacustrine cyclicity (spanning approximately 9‰ in $\delta^{13}C_{alk}$, approximately 7‰ in $\delta^{13}C_{wood}$, and approximately 15‰ in $\delta^{13}C_{toc}$) through the section, but show largely parallel trends around the ETE (Fig. 2). Specifically, there is an approximately 2–4‰ shift to ^{13}C-depleted values exactly at the ETE and associated fern spike (16) as reflected in the Newark and Hartford basins. The duration of this distinct excursion in the Newark and Hartford basins is only about 20–40 ky. This is succeeded by a distinct ^{13}C-enriched interval (by approximately

Author contributions: J.H.W. and P.E.O. designed research; J.H.W., P.E.O., and M.E.B. performed research; J.H.W., P.E.O., T.E., and R.N.S. analyzed data; and J.H.W. and P.E.O. wrote the paper.

The authors declare no conflict of interest.

See Commentary on page 6555.

[1]To whom correspondence may be addressed. E-mail: Jessica_Whiteside@Brown.edu or polsen@ldeo.columbia.edu.

This article contains supporting information online at www.pnas.org/cgi/content/full/1001706107/DCSupplemental.

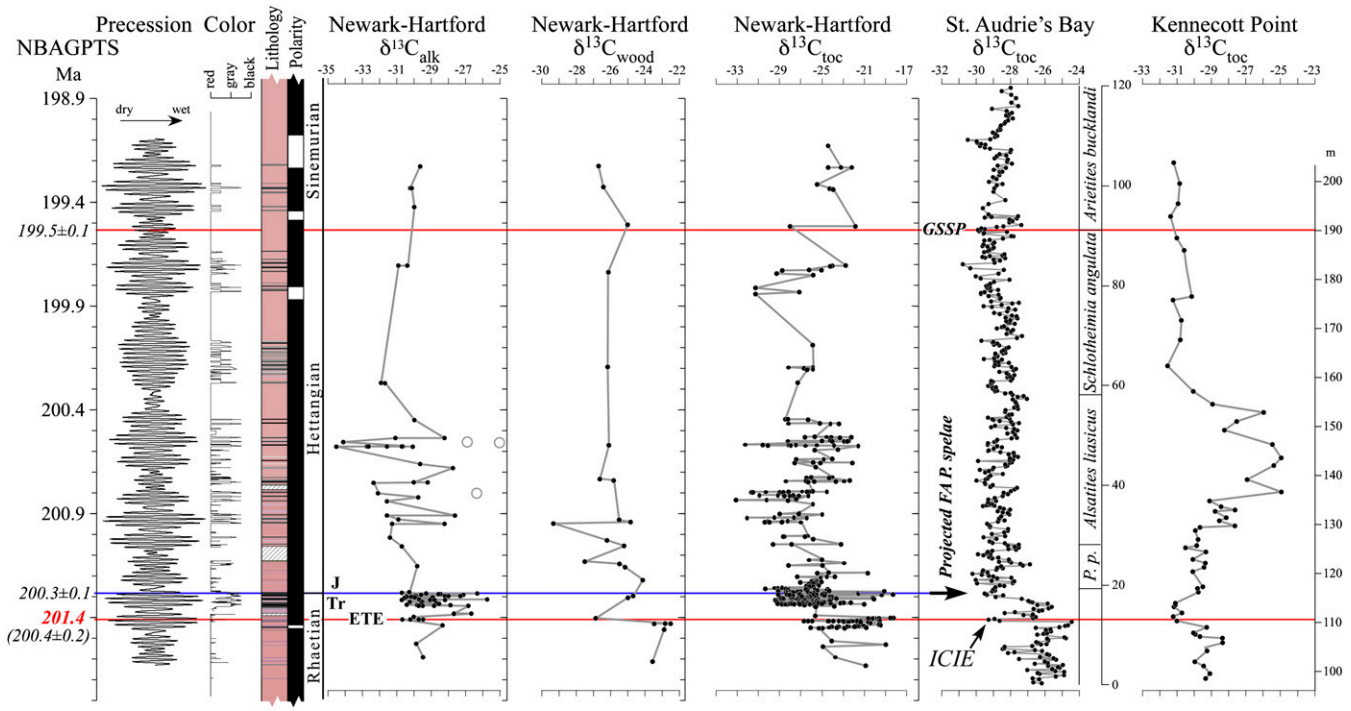

Fig. 2. Compound-specific, wood, and total organic carbon isotopes from Newark and Hartford basin strata interbedded with the CAMP lava flows (diagonal hachures) compared to marine total organic carbon ($\delta^{13}C_{toc}$) records from St. Audrie's Bay (and East Quantoxhead), United Kingdom (4, 7) and Kennecott Point, British Columbia, Canada (4). Compound-specific carbon isotopes are of the weighted mean odd C_{25}–C_{31} *n*-alkanes ($\delta^{13}C_{alk}$). Newark and Hartford sections calibrated in time with NBAGPTS (23). Dates in italics are $^{206}Pb/^{238}U$ single crystal chemically abraded-thermal ionization mass spectroscopy ages from the North Mountain Basalt of the Fundy basin (bold red) correlative with the Orange Mountain Basalt and Talcott Formation of the Newark and Hartford basins, and from marine ammonite-bearing strata from Peru (black) (from refs. 21 and 22) correlated to the St. Audrie's Bay isotope curve using the bio-and carbon isotope-stratigraphy of ref. 21. The St. Audrie's Bay and Kennecott Point data are from refs. 4 and 7 and are shown in depth with the fiducial levels of correlation (red lines) among all sections being the base of the ETE (extinction level) and the Hettangian–Sinemurian boundary constrained in the Newark and Hartford basins by paleomagnetic stratigraphy (17) (polarity) and cyclostratigraphy (from ref. 7). The blue line indicates the projected Triassic–Jurassic boundary (J/Tr) based on correlation to the first appearance datum (FA) of the ammonite *P. spelae* chosen for the marker for the base of the Hettangian at the GSSP in Kuhjoch, Austria (38) projected to the Newark and Hartford data from St. Audrie's Bay, itself correlated to Kuhjoch in ref. 39. Abbreviations are *GSSP*, global stratotype section and point for the base of the Sinemurian at St. Audrie's Bay (East Quantoxhead) (7); *ICIE*, initial carbon isotopic excursion of ref. 4; J/Tr, base of Triassic-Jurassic boundary; *P.p.*, Planorbis Zone. The gray-circles indicate rejected points in the Hartford and Newark sections because of thermal alteration or very low carbon preference index values (*SI Text*).

3–4‰) lasting another 20–40 ky, totaling about 80 ky in the negative-positive couplet. The $\delta^{13}C$ values then return to more ^{13}C-depleted values and oscillate through the rest of the record. Only the wood data seems to show any sort of distinct postcouplet pattern with a tendency to more ^{13}C-depleted values in the CAMP interval. Our carbon isotopic record below the ETE is constrained to a few hundred thousand years by an absence of strata containing organic matter.

We compared this composite record to a dataset from Late Triassic–Early Jurassic age predominantly marine strata at St. Audrie's Bay, England (Fig. 2). Previous studies of this section include a key analysis of $\delta^{13}C_{toc}$ that has framed the discussion about the cause of the ETE event (4) and more recent data that carries the isotopic record into the Sinemurian (7) (Fig. 2). This $\delta^{13}C_{toc}$ record was originally described as displaying an "initial" isotopic excursion enriched in ^{12}C beginning at the onset of the ETE, and an upper, "main" ^{12}C-enriched excursion coinciding with the first appearance datum of Jurassic ammonites (4, 20) (Fig. 2), but the data extending the section upward show conclusively that the main excursion does not exist but rather just reflects the base of a protracted interval of ^{12}C enrichment (7).

Correlation between the eastern North American continental sections and the St. Audrie's Bay marine record is afforded by independent non-carbon-isotopic means, specifically the base of the ETE below and the Hettangian–Sinemurian transition above (Fig. 2), with the interval between them being calibrated by the NBAGPTS, magneto- and cyclostratigraphy (7, 17), and radioisotopic ages (21) (*SI Text*). Given these constraints and any range of plausible accumulation rates for St. Audrie's Bay, available carbon data can be compared to the eastern North American records described here.

The accuracy of the correlation between St. Audrie's Bay and the Newark–Hartford section is corroborated by a comparison between the cyclostratigraphically defined duration of the Hettangian and radioisotopic dates from eastern North America and elsewhere. The duration of the Hettangian at St. Audrie's Bay from the projected position of the first appearance of *Psiloceras spelae* to the position of the Hettangian–Sinemurian boundary at the global stratotype section and point (GSSP) is 1.8 m.y. (7). If the age of the projected position of *P. spelae* in the Newark–Hartford section is placed at 100 ky after the age of the oldest eastern North American basalt (i.e., 201.3 Ma) the cyclostratigraphic age of the Hettangian–Sinemurian boundary (based on the correlations to the GSSP in ref. 7) is 199.5 Ma, in complete agreement with the independent marine radioisotopic age (22), which again yields a duration of 1.8 m.y. ($201.3 - 199.5 = 1.8$).

Our $\delta^{13}C_{alk}$ measurements from St. Audrie's Bay (*SI Text*) track for the most part variations in $\delta^{13}C_{toc}$ in the initial excursion (Fig. 4) and, like the $\delta^{13}C_{toc}$ (7), appear cyclical. However, the initial excursion is unusual because the C_{25} *n*-alkane is the most abundant and the most ^{13}C-depleted in the samples (*SI Text*). Given that all of the St. Audrie's samples share the same postdepositional history, this difference is most simply explained as

a change in contribution of different organisms, a possibility suggested for the origin of the initial excursion at other localities (6). Thus, a change in community structure is likely responsible for at least part of the initial excursion as seen at the St. Audrie's Bay section. This interval shows an unusual abundance of fern spores but no exceptional concentration of organic-walled aquatic organisms at St. Audrie's Bay (20), suggesting a terrestrial ecosystem change. The duration of the initial excursion at St. Audrie's Bay has been independently estimated at 20–40 ky (7) in agreement with our estimates based on the Newark–Hartford data.

The initial excursion thus can be identified as beginning at the extinction level in the Newark basin possibly extending through the time of the deposition of the oldest CAMP lava flows. Critically, extinctions persist into strata postdating the initial excursion (e.g., conodonts) at St. Audrie's Bay (20) and elsewhere, demonstrating that extinctions persisted a short time after the initial CAMP pulse.

Discussion

Both the combined Newark and Hartford $\delta^{13}C_{alk}$ and the St. Audrie's Bay $\delta^{13}C_{alk}$ data exhibit oscillations in values younger and older than the initial excursion that are not directly connected with extinctions, but rather track the lacustrine cyclicity and exhibit coherent power around an approximately 100 ky periodicity (Fig. 3) (*SI Text*). $\delta^{13}C_{alk}$ and $\delta^{13}C_{toc}$ are also coherent around approximately 100 ky. The magnitude of these oscillations decreases after the positive excursion following the initial excursion, and we suggest they reflect climate-related ecological changes altering both the taxonomic composition of the plant communities supplying the waxes and the isotopic discrimination of the members of the community under highly stressed conditions. With only the two available fiducials (the ETE and the Sinemurian–Hettangian boundary), the St. Audrie's $\delta^{13}C_{alk}$ and $\delta^{13}C_{toc}$ data also exhibit coherent approximately 100 ky periodicity using the NBAGPTS for temporal constraints. The thickness periodicities are also fully consistent with those seen in $\delta^{13}C_{toc}$, percent total organic carbon, and percent carbonate described in ref. 7 (Fig 3), again very strongly suggesting that both the time scale and the correlation between the two sections are correct.

Although the isotopic excursion and ETE predate the onset of CAMP in the Newark and Hartford basins, the lava flows in these basins do not reflect the full temporal extent of the eruptions. The Culpeper basin of Virginia and Argana and Central High Atlas basins of Morocco demonstrate that the CAMP eruptions were more extensive than the three flow sequences preserved in the Newark and Hartford basins (23) (Fig. 4). In addition, some CAMP flows in Morocco are most likely slightly older than those recognized in eastern North America (24, 25) (*SI Text*). These older flows may be synchronous with the initiation of the ETE.

It is unlikely that the initial excursion seen at St. Audrie's Bay and in eastern North America was generated by mantle CO_2 alone, because of the similarity in atmospheric and mantle $\delta^{13}C$ values (26). Hence, an injection of ^{12}C carbon from CAMP-triggered methane clathrates (4, 9) dissociation or thermogenic methane (27) release from intrusive metamorphism (13) has been hypothesized. One alternative is that an intensification of the hydrological cycle, as a result of greater CO_2-forced warming causing an increase in available moisture driving greater isotopic discrimination (28) caused a shift toward more ^{13}C-depleted values in the plant wax *n*-alkanes. This is entirely consistent with the enhanced lacustrine cyclicity and *n*-alkane cyclicity in the Newark and Hartford data after the ETE. A concurrent shutoff of the biological pump would result in a homogenization of the water column caused by the extinction of zooplankton grazers (cf. K-T boundary in ref. 29) with surface waters becoming enriched in ^{12}C. The short duration of the initial excursion is also incompatible with the modeled estimates of the

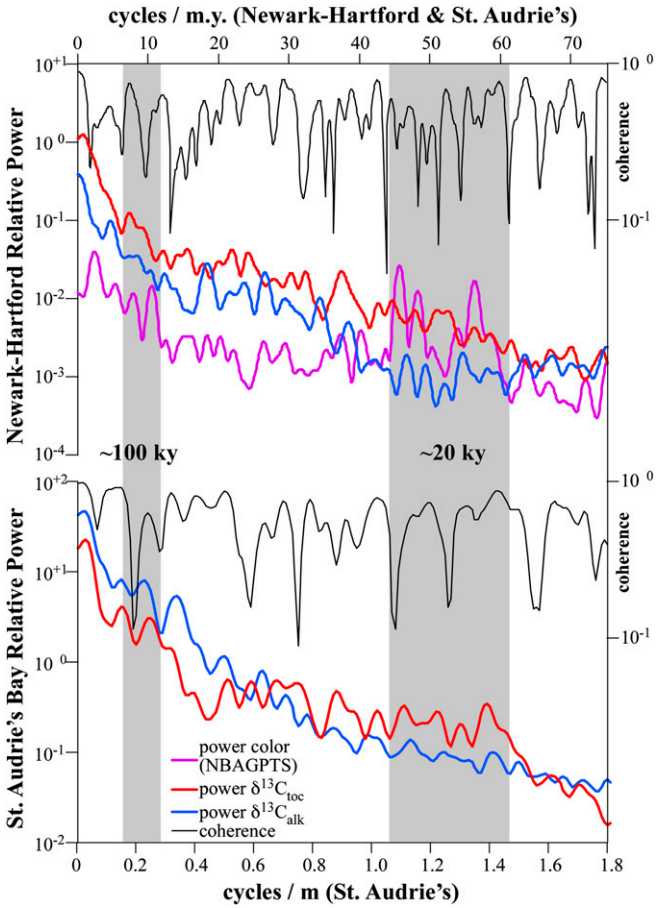

Fig. 3. Comparison between power spectra of carbon isotopic data from the Newark and Hartford basins and the St. Audrie's Bay section using the same time scale (NBAGPTS) based on the correlation to the base of the ETE and the Hettangian–Sinemurian boundary. Note the correspondence between the approximately 100 ky periods in $\delta^{13}C_{alk}$ and $\delta^{13}C_{toc}$ in both the Newark–Hartford and St. Audrie's data and the presence of the approximately 20 ky cycle in the St. Audrie's $\delta^{13}C_{toc}$ data. Coherence in the Newark–Hartford data and in the St Audrie's data is shown between the $\delta^{13}C_{alk}$ and $\delta^{13}C_{toc}$ with the spectrum for color shown for reference as it is tuned to the NBAGPTS. Nonzero coherence is greater than 0.6.

recovery time from a methane clathrates dissociation event by over an order of magnitude (20–40 ky compared to 700–1000 ky from ref. 26). Other proposed killing mechanisms include CAMP-outgassed or metamorphism-related volatiles such as sulfuric acid (27) or halogens (13, 30); however, none of these models have yielded unique predictions testable in the sedimentary record. We also cannot exclude a role for a bolide impact as a killing mechanism, although evidence consisting mostly of modest Ir anomalies (16) is also compatible with a volcanic origin.

Carbonate $\delta^{13}C$ records from St. Audrie's Bay (31) track the $\delta^{13}C_{toc}$ and $\delta^{13}C_{alk}$ data, which in turn match the variations in the Newark and Hartford $\delta^{13}C_{alk}$ data that are orbitally paced. Because the St. Audrie's Bay carbonate data are unlikely to have been affected by local community change without some process linking them via the exchangeable carbon reservoirs, there seems to have been a significant role for orbital cycles pacing the Earth's exchangeable reservoirs as has been suggested for a number of other isotopic excursions (32). However, the behavior of *n*-alkanes in the initial excursion is qualitatively different from the other fluctuations, suggesting a different origin such as the effects of the initial influx of greenhouse gases and the extinctions themselves, the exact expression of which would be influenced by synergetic changes in the local conditions and local communities

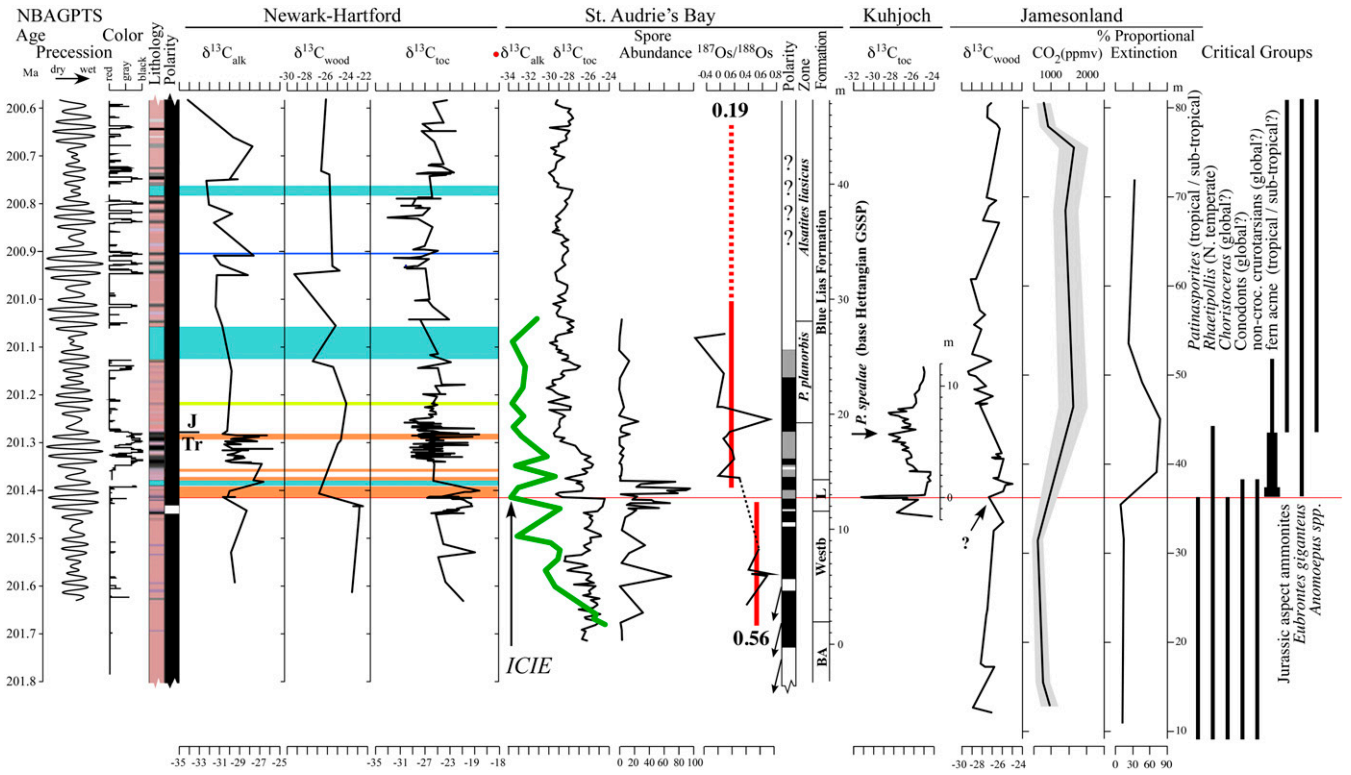

Fig. 4. Detailed comparison and correlation between the Newark and Hartford compound-specific carbon isotopes of the weighted mean odd C25–C31 *n*-alkanes ($\delta^{13}C_{alk}$) from lacustrine rocks interbedded with the CAMP flood basalt flows (from Fig. 2) with environmentally and biological relevant data from other sections. These are new compound-specific carbon isotopes of the weighted mean odd C_{25}–C_{31} *n*-alkanes ($\delta^{13}C_{alk}$) from St. Audrie's Bay and total organic carbon ($\delta^{13}C_{toc}$) data from refs. 4 and 7, Os isotopic data from ref. 33, and paleomagnetic polarity stratigraphy from ref. 20, all from St. Audrie's Bay; carbon isotope data from wood ($\delta^{13}C_{wood}$) (9), leaf stomatal density proxy data for CO_2 (9) and floral species extinction rate [Proportional Extinction (%)] from Jamesonland, Greenland (Astartekløft); and the ranges of critical taxa (pollen, *Patinasporites* and *Rhaetipollis*, cited in refs. 16 and 20), invertebrates (*Choristoceras*) (4, 35), conodonts (20), "Jurassic aspect" ammonites including *P. spelae* (35) and *P. planorbis* (20), and tetrapod footprint (16) (noncrocodylomorph crurotarsans) (e.g., *Brachychirotherium* and *Apatopus* and the large theropod dinosaur track *Eubrontes giganteus*). CAMP basalt flows in the Newark and Hartford basins are indicated by the light blue-green bars (flows) and a basaltic ash by a dark blue bar (Pompton Tuff, *SI Text*), while other CAMP basalt flows are shown in orange for the Central High Atlas from Morocco (24, 25), and yellow for the Culpeper basin (Virginia) (23). Jamesonland data correlated to St. Audrie's Bay and Newark and Hartford sections by the initiation of the plant extinctions (terrestrial ETE) and wood isotopic records. Abbreviations are as in Fig. 2 with the addition of BA, Blue Anchor Formation; L, Lilstock Formation; and Westb, Westbury Formation.

(e.g., ref. 6). The long-term maintenance of relatively ^{13}C-depleted average values in the Jurassic for at least the length of the Hettangian and early Sinemurian are plausibly the result of nonorbital changes, such as a long-term change in the biological pump, perhaps related to the extinction itself (e.g., ref. 29).

Our data also allow isotopic, CO_2 proxy, and floral data from Jamesonland, Greenland (9) to be compared to Newark and Hartford data and the CAMP (Fig. 4). The ^{13}C-depleted interval in the Jamesonland $\delta^{13}C_{wood}$ data plausibly corresponds to a similar interval seen in the Newark and Hartford $\delta^{13}C_{wood}$ data and the interval of CAMP flows in eastern North America and Morocco. In contrast, concentrated floral extinctions are limited to the older CAMP flows. Given this correlation, the interval of elevated CO_2 based on plant stomatal data corresponds nearly exactly to the CAMP episode, strongly supporting a direct role for the eruptions.

Osmium isotopic data from St. Audrie's Bay (33) (Fig. 4) agree with this interpretation and suggest that the CAMP was supplying weathering products to the ocean very soon after the initiation of eruption shortly after the ETE. $^{187}Os/^{188}Os$ values shift about 0.4 from higher to lower values over the ETE, suggesting an input of unradiogenic Os of mantle (or extraterrestrial) origin or a reduction of continentally derived Os or both, but the fact that Os concentrations increase over the same interval (33) suggests the former, namely the weathering products of the CAMP.

Conclusions

With this correlation of isotopic excursions and marine stratigraphy to the CAMP, it is possible to refine the sequence of marine and continental biotic events in relation to the eruptions (Fig. 4). The onsets of marine and continental extinctions were simultaneous with each other and the initial excursion, with the input of CO_2 leading to an oceanic biocalcification crisis (10). In the northern tropics, the continental extinction is extremely abrupt with the disappearance of about 50% of the palynoflora and a synchronous extinction among tetrapods (16). Subsequently, there was a regional fern spike followed by macrofossil first appearances of several fern taxa and cheirolepidaceous conifers with adaptations for environmental stress (34) coupled with a flood of the pollen species *Classopollis meyeriana* (23) [seen also in higher latitudes (35)]: These overlap the known approximately 300 ky eruptive maximum of CAMP (23). Footprint evidence indicates that theropod dinosaurs abruptly increased in size and relative abundance during this time (16). This is followed by a slow return to larger leaved cheirolepidaceous conifers and different species of *Classopollis*, comprising a late Hettangian floral recovery about 1 m.y. after the beginning of the initial excursion and directly following ^{13}C-enriched interval.

Our *n*-alkane data also reveal changes in the contributing organisms that vary both temporally and geographically, as would be expected of a community response to a significant increase in temperature and/or humidity caused by enhanced CO_2 forcing (36).

The negative $\delta^{13}C$ excursions in the Newark, Hartford, and St. Audrie's Bay documented by the *n*-alkane, wood, total organic carbon data, and the correlations to Jamesonland strongly suggest a massive input of ^{13}C-depleted CO_2 and/or other greenhouse gases coincident with the onset of CAMP. The very tight association between the onset of the CAMP and the abrupt extinctions in the tropics and subtropics, the more protracted extinctions well into the CAMP episode in the higher latitudes during the time of maximum eruptive rate, and the association of the elevated CO_2 levels tied to the entire known CAMP episode strongly argues for a major causative role for CAMP-generated CO_2 in the extinctions themselves. Our interpretation of the carbon isotopic data from these continental and marine sections provides strong direct evidence by direct superposition that the eruption of a giant flood basalt province could cause a climatic catastrophe resulting in a major mass extinction.

Methods

For *n*-alkane extraction, approximately 4–12 g of powdered sedimentary rock samples were extracted on a Dionex Accelerated Solvent Extraction system using three washes of dichloromethane (DCM) or 9:1 DCM/methanol to produce a total lipid extract (TLE). The TLE was saponified with 0.5N KOH/methanol, and then extracted with hexane. This neutral extract was dried with anhydrous Na_2SO_4 to remove traces of water, then eluted from a silica gel column (1 mL bed volume, silica gel 2% deactivated) into two fractions, first a hexane elutable and second a combined DCM and methanol elutable fraction. If required, the hexane elutable fraction was further fractionated into adduct [straight chain ($C \geq 14$) *n*-alkanes] and nonadduct fractions by urea adduction, or by sequestering the straight chain alkanes in zeolites, rinsing with hexane, and alkane recovery by dissolution of the zeolite with aqueous HF.

Compound-specific carbon isotopic measurements were determined by isotope ratio monitoring–gas chromatography/mass spectrometry using a Thermo DeltaVPlus MS coupled to an Agilent 6890 GC via a GCC-III combustion interface at Brown University. The $\delta^{13}C$ values for individual compounds were determined based on introduction of reference CO_2 gas pulses (previously and subsequently calibrated with a series of well-characterized standard materials), reported as means of duplicate runs ($\sigma = \pm 0.3$ to 0.6), and expressed in ‰ relative to the Pee Dee belemnite (PDB). The bulk organic matter of sediment wood was analyzed to determine the ratio of $^{13}C/^{12}C$ by mass spectrometry. The samples were cleaned with deionized water, air-dried, ground into a fine powder with a ceramic mortar and pestle, fumed with 37% HCl in a bell jar at 60 °C for 50 h (to remove recalcitrant carbonate), and dried above a plate of silica gel desiccant at 60 °C for at least 24 h. All samples were weighed into silver capsules, with mass determined by total organic-carbon (TOC) content, grouped according to TOC, and processed with an automated micro-Dumas combustion technique using a Europa ANCA system plumbed into a 20-20-NT continuous flow mass spectrometer system at Lamont-Doherty Earth Observatory. C isotope ratios were measured against National Institute of Standards and Technology and International Atomic Energy Agency standard reference materials and combusted in the same manner as the samples (glucosamine, $\delta^{13}C = -20.80$, $C = 20.50\%$; methionine, $\delta^{13}C = 25.10$, $C = 40.25\%$ (Cornell only), all versus the PDB ($^{13}C/^{12}C = 11237.2 \pm 60 \times 10^{-6}$). Precision of the analytical system is 0.12‰ for C at the typical sample sizes (4 μm C) used here.

Time series analysis was performed using Analyseries 2.037 (37).

ACKNOWLEDGMENTS. We thank Daniel Montluçon, Carl Johnson, and Camly Tran for laboratory assistance. We are grateful to Micha Ruhl for permission to use the St. Audrie's Bay δ13C curve from refs. 7 and 19. We also thank Michael Rampino and Randall Irmis for reviewing the manuscript. J.H.W. and P.E.O. acknowledge support from the US National Science Foundation (Grant EAR 0801138 to J.H.W. and Grant EAR 0753496 to P.E.O.).

1. Farquhar GD, Ehleringer JR, Hubick KT (1989) Carbon isotope discrimination and photosynthesis. *Annu Rev Plant Physiol Plant Mol Biol* 40:503–537.
2. Eglinton G, Hamilton RJ (1967) Leaf epicuticular waxes. *Science* 156:1322–1335.
3. Marzoli A, et al. (1999) Extensive 200-million-year-old continental flood basalts of the Central Atlantic Magmatic Province. *Science* 284:616–618.
4. Hesselbo SP, et al. (2002) Terrestrial and marine extinction at the Triassic-Jurassic boundary synchronized with major carbon-cycle perturbation: A link to initiation of massive volcanism?. *Geology* 30:251–254.
5. Williford KH, et al. (2007) An extended stable organic carbon isotope record across the Triassic-Jurassic boundary in the Queen Charlotte Islands, British Columbia, Canada. *Palaeogeogr Palaeocl* 244:290–296.
6. Kürschner WM, Bonis NR, Krystyn L (2007) Carbon-isotope stratigraphy and palynostratigraphy of the Triassic-Jurassic transition in the Tiefengraben section -Northern Calcareous Alps (Austria). *Palaeogeogr Palaeocl* 244:257–280.
7. Ruhl M, et al. Astronomical constraints on the duration of the Early Jurassic Hettangian stage and recovery rates following the end-Triassic mass extinction (St. Audrie's Bay/East Quantoxhead, UK). *Earth Planet Sci Lett*, in press.
8. Benton MJ (1995) Diversification and extinction in the history of life. *Science* 268:52–58.
9. McElwain JC, Wagner PJ, Hesselbo SP (2009) Fossil plant relative abundances indicate sudden loss of Late Triassic biodiversity in East Greenland. *Science* 324:1554–1556.
10. van de Schootbrugge B, et al. (2007) End-Triassic calcification crisis and blooms of organic-walled 'disaster species'. *Palaeogeogr Palaeocl* 244:126–141.
11. Rampino MR, Stothers RB (1988) Flood basalt volcanism during the past 250 million years. *Science* 241:663–668.
12. Wignall PB (2001) Large igneous provinces and mass extinctions. *Earth-Sci Rev* 53:1–33.
13. Ganino C, Arndt NT (2009) Climate changes caused by degassing of sediments during the emplacement of large igneous provinces. *Geology* 37:323–326.
14. Kent DV, Tauxe L (2005) Corrected Late Triassic latitudes for continents adjacent to the North Atlantic. *Science* 307:240–244.
15. Kent DV, Olsen PE (1999) Astronomically tuned geomagnetic polarity time scale for the Late Triassic. *J Geophys Res* 104:12831–12841.
16. Olsen PE, et al. (2002) Ascent of dinosaurs linked to an iridium anomaly at the Triassic-Jurassic boundary. *Science* 296:1305–1307.
17. Kent DV, Olsen PE (2008) Early Jurassic magnetostratigraphy and paleolatitudes from the Hartford continental rift basin (eastern North America): Testing for polarity bias and abrupt polar wander in association with the central Atlantic magmatic province. *J Geophys Res* 113:B06105 doi: 10.1029/2007JB005407.
18. Muttoni G, et al. (2004) Tethyan magnetostratigraphy from Pizzo Mondello (Sicily) and correlation to the Late Triassic Newark astrochronological polarity time scale. *Geol Soc Am Bull* 116:1043–1058.
19. Ruhl M (2010) Carbon cycle changes during the Triassic–Jurassic transition. *Laboratory of Paleobotany and Palynology, Contribution Series 28* (Utrecht Univ, The Netherlands).
20. Hounslow MW, Posen PE, Warrington G (2004) Magnetostratigraphy and biostratigraphy of the Upper Triassic and lowermost Jurassic succession, St. Audrie's Bay, UK. *Palaeogeogr Palaeocl* 213:331–358.
21. Schoene B, et al. A correlation between the Triassic-Jurassic boundary mass extinction and flood basalt eruption at the 100 ka-level using ID-TIMS U/Pb zircon geochronology. *Geology*, in press.
22. Schaltegger U, et al. (2008) Precise U-Pb age constraints for end-Triassic mass extinction, its correlation to volcanism and Hettangian postextinction recovery. *Earth Planet Sci Lett* 267:266–275.
23. Whiteside JH, et al. (2007) Synchrony between the CAMP and the Triassic-Jurassic mass-extinction event?. *Palaeogeogr Palaeocl* 244:345–367.
24. Marzoli A, et al. (2004) Synchrony of the Central Atlantic magmatic province and the Triassic-Jurassic boundary climatic and biotic crisis. *Geology* 32:973–976.
25. Deenen MHL, et al. (2010) A new chronology for the end-Triassic mass extinction. *Earth Planet Sci Lett* 291:113–125.
26. Beerling DJ, Berner RA (2002) Biogeochemical constraints on the Triassic-Jurassic boundary carbon cycle event. *Global Biogeochem Cycles* 16:10-1–10-16 doi: 10.1029/2001GB001637.
27. van de Schootbrugge B, et al. (2009) Floral changes across the Triassic/Jurassic boundary linked to flood basalt volcanism. *Nat Geosci* 2:589–594.
28. Bowen GJ, et al. (2004) A humid climate state during the Palaeocene/Eocene thermal maximum. *Nature* 432:495–499.
29. D'Hondt SD (2005) Consequences of the Cretaceous/Paleogene mass extinction for marine ecosystems. *Annu Rev Ecol Evol Syst* 36:295–317.
30. Svensen H, et al. (2009) Siberian gas venting and the end-Permian environmental crisis. *Earth Planet Sci Lett* 277:490–500.
31. Korte C, et al. (2009) Paleoenvironmental significance of carbon-and oxygen-isotope stratigraphy of marine Triassic-Jurassic boundary sections in SW Britain. *J Geol Soc London* 166:431–445.
32. Kemp DB, et al. (2005) Astronomical pacing of methane release in the Early Jurassic Period. *Nature* 437:396–399.
33. Cohen AS, Coe AL (2002) New geochemical evidence for the onset of volcanism in the Central Atlantic Magmatic Province and environmental change at the Triassic-Jurassic boundary. *Geology* 30:267–270.
34. Cornet B (1977) The palynostratigraphy and age of the Newark Supergroup. PhD thesis (Pennsylvania State Univ, University Park, PA).
35. Bonis NR, et al. (2009) Climate change driven black shale deposition during the end-Triassic in the western Tethys. *Palaeogeogr Palaeocl* doi: 10.1016/j.palaeo.2009.06.016.
36. Smith FA, et al. (2007) Magnitude of the carbon isotope excursion at the Paleocene-Eocene thermal maximum: The role of plant community change. *Earth Planet Sci Lett* 262:50–65.
37. Paillard D, Labeyrie L, Yiou P (1996) Macintosh program performs time-series analysis. *Eos Trans AGU* 77:379.
38. Morton N (2008) Details of voting on proposed GSSP and ASSP for the base of the Hettangian Stage and Jurassic System. *Int Subcomm Jurassic Stratigr Newslett*, 35 p:74.
39. Ruhl M, Kürschner WM, Krystyn L (2009) Triassic–Jurassic organic carbon isotope stratigraphy of key sections in the western Tethys realm (Austria). *Earth Planet Sci Lett* 281:169–187.